RSC Advances

ROYAL SOCIETY OF CHEMISTRY

www.rsc.org/advances

Journal Name

ARTICLE

Synthesis, crystal structure, fluorescence and antimicrobial activity of a series of rare-earth complexes based on indolebutyric acid

Received 00th January 20xx,
Accepted 00th January 20xx

DOI: 10.1039/x0xx00000x

www.rsc.org/

Zhi-Nan Wang,[a] Xue-Ting Xu,[a] Xiao Lv,[b] Feng-Ying Bai,[a*] Shu-Qing Liu[b*] and Yong-Heng Xing[a]

A series of lanthanide complexes, namely $[Ln(IBA)_3(phen)]\cdot(Hphen)\cdot NO_3\cdot xH_2O\cdot yEtOH$ (**1-6**) (Ln=La(**1**), x=1, y=0.5; Pr(**2**), x=2, y=0; Eu(**3**), x=2, y=0; Gd(**4**), x=2, y=0; Tb(**5**), x=1.5, y=0; Yb(**6**), x=2, y=0. IBA= indole-3-butyric acid, phen= 1,10-phenanthroline), $[Sm(IBA)_2(phen)_2]\cdot NO_3$ (**7**) and $Ln(IBA)_3(phen)$ (**8-10**) (Ln=Eu(**8**); Tb(**9**); Yb(**10**)), have been successfully synthesized. All complexes were characterized by elemental analysis, IR spectroscopy, UV-vis spectroscopy, thermal gravimetric technology, powder X−ray diffraction and single-crystal X-ray diffraction. Structural analyses reveal that each lanthanide atom held distorted tricapped trigonal prism geometry with a nine-coordinate mode in complexes **1-9** and held bicapped trigonal prism geometry with an eight-coordinate mode in complex **10**. There are three kinds of coordination modes of IBA ligands in complexes **1-6** and **8-9**: a μ_1-η^1:η^1 bidentate chelating mode, a μ_2-η^1:η^1 double monodentate bridging mode and a μ_2-η^1:η^2 bridging mode. For complex **7**, there are two kinds of coordination mode of IBA ligands: a μ_2-η^1:η^1 and a μ_2-η^1:η^2 bridging modes. For complex **10**, there are also two kinds of coordination mode of IBA ligands, a μ_2-η^1:η^1 double monodentate bridging mode and a μ_1-η^1:η^1 bidentate chelating mode. Adjacent lanthanide atoms were linked via the μ_2-bridging carboxylate groups of the IBA ligands to generate a binuclear building unit. In addition, their photoluminescent characterization and antimicrobial activity against the fungi *Golden Staph* (G.S), *Pseudomonas Aeruginosa* (P.A), *Escherichia Coli* (E.C), *Bacillus Subtillis* (B.S) and *Candida Albicans* (C.A) were studied firstly.

Introduction

Lanthanide complexes have attracted intense interest due to the potential application in luminescence, sensors, magnetism, catalysis activity, gas storage, ion exchange and biologic activity [1]. The combination of lanthanide atoms and the different organic ligands can produce various crystal architectures. It is worth to mention that the characteristic of the organic ligands play a key role in the construction of complexes. Among the complexes with the ligands of aromatic carboxylic acid reported by predecessors, such as $[Tb(BTB)(H_2O)]\cdot 2(C_6H_{12}O)$ (BTB=1,3,5-benzenetrisbenzoate) [2], $Ce(SSA)(H_2O)_2$ (SSA=sulfonic salicylic acid) [3], $[Tb(btc)(H_2O)]\cdot(H_2O)_{0.5}DMF$ (btc=1,3,5-benzenetricarboxylates) [4], $[Dy(btc)(H_2O)]\cdot DMF$ [5], $[Eu(btc)(H_2O)]\cdot(H_2O)_{1.5}$ [6] and the ligands of aliphatic carboxylic acid such as $[Nd(C_{10}H_{16}O_4)(C_{10}H_{17}O_4)(H_2O)]_n$ [7], $Yb(H_2hedp)\cdot H_2O$ (H_5hedp=etidronic acid) [8] have been synthesized. In particular, indole-3-butyric acid (IBA) is an endogenous auxin substance found in plants, it is well documented that the biological activities of IBA as substantially enhanced when it is combined with the metal ions [9]. Such complexes $Zn(IBA)_2\cdot H_2O$ and $Cu(IBA)(C_2H_5OH)_2$ have been reported earlier [10], the lanthanide complexes with indole-3-butyric acid were less reported.

In addition, it has been observed for a long time that lanthanide elements are beneficial to plant growth [11]. In this context, the antimicrobial activity of lanthanide complexes with IBA ligand may be promising in the treatment of plant infectious disease caused by fungi and bacteria. Here, a series of lanthanide complexes with IBA, namely, $[Ln(IBA)_3(phen)]\cdot(Hphen)\cdot NO_3\cdot xH_2O\cdot yEtOH$ (**1-6**) (Ln=La(**1**), x=1, y=0.5; Pr(**2**), x=2, y=0; Eu(**3**), x=2, y=0; Gd(**4**), x=2, y=0; Tb(**5**), x=1.5, y=0; Yb(**6**), x=2, y=0). IBA= indole-3-butyric acid, phen= 1,10-phenanthroline), $[Sm(IBA)_2(phen)_2]\cdot NO_3$ (**7**), $Ln(IBA)_3(phen)$ (**8-10**) (Ln=Eu(**8**); Tb(**9**); Yb(**10**)) were designed and synthesized. And all complexes were characterized by signal-crystal X-ray diffraction, IR spectra, UV-vis spectra, PXRD analysis, and the thermal properties and luminescence of them were also studied. In order to illustrate their antimicrobial

[a] College of Chemistry and Chemical Engineering Liaoning Normal University, Dalian, 116029, P.R. China.E-mail: baifengying2003@163.com
[b] Department of Biochemistry and Molecular Biology, Dalian Medical University, Dalian, 116044, P. R. China. E-mail: Lsqsmz@163.com

† Electronic Supplementary Information (ESI) available: The selected bond lengths and angles for complexes **1**-**10** are listed in Tables S1-S3. Their hydrogen bonds are shown in Table S4. Infrared spectra, UV-vis spectra, Photoluminescence spectra, TG curves and PXRD patterns are shown in Figs.S1-S43. Figs.S44-S63 have presented the molecular structures and hydrogen bonds connection mode of complexes **1-5** and **9-10**, respectively. Figs.S64-S79 have presented the antimicrobial activity against G.S, P.A, E.C and B.S of complexes and phen. Copies of this information may be obtained free of charge, by quoting the publication citation and deposition numbers CCDC 1044883-1044892 from the Director, CCDC, 12 Union Road. Cambridge, CB2 1EZ, UK (fax+44-1223-336033; e-mail: deposit@ccdc.cam.ac.uk or http://www.ccdc.cam.ac.uk). See DOI: 10.1039/x0xx00000x

activities of a series of lanthanide complexes with IBA and phen ligand, the antimicrobial activity against the fungi *Golden Staph* (G.S), *Pseudomonas Aeruginosa* (P.A), *Escherichia Coli* (E.C), *Bacillus Subtillis* (B.S) and *Candida Albicans* (C.A) were investigated in detail also.

Experimental

Materials and methods

All other chemicals purchased were of reagent grade or better and used without further purification. IR spectra were recorded on a JASCO FT/IR-480 PLUS Fourier Transform spectrometer with pressed KBr pellets in the range of 200-4000 cm^{-1}. The elemental analyses for C, H, and N were carried out on a Perkin Elmer 240C automatic analyzer. Thermogravimetric analyses (TG) were performed under the condition of N_2 atmosphere with a heating rate of 10 ºC/min on a Perkin Elmer Diamond TG/DTA. The luminescence spectra were recorded on a JASCO F-6500 spectrofluorimeter (solid). UV-vis spectra were recorded on JASCO V-570 spectrometer (200-2500 nm, in form of solid sample). Powder X-ray diffraction (PXRD) patterns were obtained on a Bruker Advance-D8.

Antimicrobial activity-materials and methods

All the synthesized complexes were tested for their antimicrobial activities against a large number of standard microorganism of *Golden Staph* (G.S), *Pseudomonas Aeruginosa* (P.A), *Escherichia Coli* (E.C), *Bacillus Subtillis* (B.S) and *Candida Albicans* (C.A) in vitro, representatively. The starting ligands (IBA and 1,10-phen) and metal salts $Ln(NO_3)_3{\cdot}6H_2O$ and $LnCl_3{\cdot}6H_2O$ were also included for a comparison. All the compounds were dissolved in dimethylsulfoxide (DMSO) to prepare four different concentrations (20, 10, 5, 2.5 mg/ml) for evaluation of dose response. The bacterial strains were grown on nutrient agar at 37 °C for 17 h. The bacterial suspensions were measured the absorbance at 600 nm and diluted to OD_{600} = 0.1 (8.5×10^9 CFU/L). The suspension was used to inoculate sterile Petri plates of 9.0 cm diameter in which the test organisms were grown. After solidification, a hole of diameter of 0.6 cm was pierced by a sterile cork borer. Antibacterial activities of the complexes and ligands were evaluated by measuring the inhibition zone diameters (IZD). Each of the above experiments was repeated thrice along with a control set using DMSO and the mean value was taken for comparison.

Treatment the DNA of the E.C with the samples

The DNA of E.C (3.5 µL) was added into the solution of complex **2** with three different concentrations (6, 8, 10 mg/ml), the DNA maker and DMSO were tested for comparison. The sample was taken at 37 °C for 2 h, and after the agarose gel electrophoresis, the DNA cleavage of E.C was observed under UV transilluminator.

Preparation of the complexes

Complexes $[Ln(IBA)_3(phen)]{\cdot}(Hphen){\cdot}NO_3{\cdot}xH_2O{\cdot}yEtOH$ (1-6) (Ln=La(1), x=1, y=0.5; Pr(2), x=2, y=0; Eu(3), x=2, y=0; Gd(4), x=2, y=0; Tb(5), x=1.5, y=0; Yb(6), x=2, y=0) A solution containing IBA (0.15 g, 0.75 mmol) and phen (0.10 g, 0.50 mmol) in ethanol (95%, 10 mL) was added drop-wise to a solution of $Ln(NO_3)_3{\cdot}6H_2O$ (0.11 g, 0.25 mmol) in deionized water (10 mL). The reaction mixture was stirred for 4 h and the solution was then left for several days at room temperature. Complexes **1-6** were obtained and also difficult to dissolve in water and common organic solvents except for DMSO and DMF.

$C_{61}H_{58}N_8O_{10.5}La$ (**1**): Yield: (based on La^{3+}): 49.5%. Analysis: (Anal. Calc. for $C_{61}H_{58}N_8O_{10.5}La$: C, 60.49; H, 4.79; N, 9.25%; Found: C, 60.40; H, 4.75; N, 9.24%). IR spectrum (KBr, ν, cm^{-1}): 3406($\nu_{N\text{-}H}$); 3211($\nu_{O\text{-}H}$); 3057($_{Ar\text{-}H}$); 2929, 2869($\nu\text{-}_{(CH2)}$-); 1588 ($\nu_{asCOO\text{-}}$); 1428($\nu_{sCOO\text{-}}$); 1519($\nu_{C=N}$); 1496($\nu_{C=C}$); 1385(ν_{NO3}^-); 1190 ($\nu_{C\text{-}C}$); 1102($\nu_{C\text{-}N}$); 1048($\nu_{C\text{-}O}$); 845, 746, 731($\delta_{Ar\text{-}H}$); 429($\nu_{La\text{-}O}$).

$C_{60}H_{57}N_8O_{11}Pr$ (**2**): Yield: (based on Pr^{3+}): 61.7%. Analysis: (Anal. Calc. for $C_{60}H_{57}N_8O_{11}Pr$: C, 59.65; H, 4.72; N, 9.28%; Found: C, 59.60; H, 4.77; N, 9.32%). IR spectrum (KBr, ν, cm^{-1}): 3407($\nu_{N\text{-}H}$); 3212($_{O\text{-}H}$); 3056($_{Ar\text{-}H}$); 2929, 2868($\nu\text{-}_{(CH2)}$-); 1583 (ν_{asCOO}^-); 1429(ν_{sCOO}^-); 1514($\nu_{C=N}$); 1496($\nu_{C=C}$); 1385(ν_{NO3}^-); 1190 ($\nu_{C\text{-}C}$); 1101($\nu_{C\text{-}N}$); 1028($\nu_{C\text{-}O}$); 845, 746, 731($\delta_{Ar\text{-}H}$); 429($\nu_{Pr\text{-}O}$).

$C_{60}H_{57}N_8O_{11}Eu$(**3**): Yield: (based on Eu^{3+}): 53.9%. Analysis: (Anal. Calc. for $C_{60}H_{57}N_8O_{11}Eu$: C, 59.11; H, 4.68; N, 9.19%; Found: C, 59.15; H, 4.75; N, 9.22%). IR spectrum (KBr, ν, cm^{-1}): 3406($\nu_{N\text{-}H}$); 3212($_{O\text{-}H}$); 3056($_{Ar\text{-}H}$); 2929, 2869($\nu\text{-}_{(CH2)}$-); 1584 ($\nu_{asCOO\text{-}}$); 1429 (ν_{sCOO}^-); 1515($_{C=N}$); 1496($\nu_{C=C}$); 1385(ν_{NO3}^-); 1190 ($\nu_{C\text{-}C}$); 1101 ($\nu_{C\text{-}N}$); 1028($\nu_{C\text{-}O}$); 845, 746, 731($\delta_{Ar\text{-}H}$); 429 ($\nu_{Eu\text{-}O}$).

$C_{60}H_{57}N_8O_{11}Gd$ (**4**): Yield: (based on Gd^{3+}): 46.7%. Analysis: (Anal. Calc. for $C_{60}H_{57}N_8O_{11}Gd$: C, 58.85; H, 4.66; N, 9.15%; Found: C, 58.80; H, 4.72; N, 9.12%). IR spectrum (KBr, ν, cm^{-1}): 3407($\nu_{N\text{-}H}$); 3212($_{O\text{-}H}$); 3057($_{Ar\text{-}H}$); 2930, 2869($\nu\text{-}_{(CH2)}$-); 1587 ($\nu_{asCOO\text{-}}$); 1429(ν_{sCOO}-); 1518($\nu_{C=N}$); 1496($\nu_{C=C}$); 1385(ν_{NO3}^-); 1191 ($\nu_{C\text{-}C}$); 1102($\nu_{C\text{-}N}$); 1038($\nu_{C\text{-}O}$); 845, 746, 731($\delta_{Ar\text{-}H}$); 429($\nu_{Gd\text{-}O}$).

$C_{60}H_{56}N_8O_{10.5}Tb$(**5**): Yield: (based on Tb^{3+}): 55.8%. Analysis: (Anal. Calc. for $C_{60}H_{56}N_8O_{10.5}Tb$: C, 58.21; H, 4.61; N, 9.21%; Found: C, 58.27; H, 4.65; N, 9.24%). IR spectrum (KBr, ν, cm^{-1}): 3406($\nu_{N\text{-}H}$); 3215($\nu_{O\text{-}H}$); 3057($_{Ar\text{-}H}$); 2930, 2869($\nu\text{-}_{(CH2)}$-); 1587 ($\nu_{asCOO\text{-}}$); 1427($\nu_s$coo-); 1519$\nu_{C=N}$); 1496($\nu_{C=C}$); 1385(ν_{NO3}^-); 1190 ($\nu_{C\text{-}C}$); 1102($\nu_{C\text{-}N}$); 1028($\nu_{C\text{-}O}$); 844, 746, 731($\delta_{Ar\text{-}H}$); 429($\nu_{Tb\text{-}O}$).

$C_{60}H_{57}N_8O_{11}Yb$(**6**): Yield: (based on Yb^{3+}): 57.3%. Analysis: (Anal. Calc. for $C_{60}H_{57}N_8O_{11}Yb$: C, 58.10; H, 4.60; N, 9.04%; Found: C, 58.06; H, 4.52; N, 9.07%). IR spectrum (KBr, ν, cm^{-1}): 3407($\nu_{N\text{-}H}$); 3213($_{O\text{-}H}$); 3057($_{Ar\text{-}H}$); 2930, 2869($\nu\text{-}_{(CH2)}$-); 1586 ($\nu_{asCOO\text{-}}$); 1429(ν_{sCOO}-); 1516($\nu_{C=N}$); 1496($\nu_{C=C}$); 1385(ν_{NO3}^-); 1190 ($\nu_{C\text{-}C}$); 1102($\nu_{C\text{-}N}$); 1029($\nu_{C\text{-}O}$); 845, 746, 731($\delta_{Ar\text{-}H}$); 429 ($\nu_{Yb\text{-}O}$).

Complex $[Sm(IBA)_2(phen)_2]{\cdot}NO_3$ (7) A solution containing IBA (0.09 g, 0.50 mmol) and phen (0.10 g, 0.50 mmol) in ethanol (95%, 10 mL) was added drop-wise to a solution of $Sm(NO_3)_3{\cdot}6H_2O$ (0.11 g, 0.25 mmol) in deionized water (5 mL). The pH was adjusted to 6 using a solution of NaOH (1 M) and the reaction mixture was stirred for 4 h. After the solution was left for 5 days at room temperature, light yellow needle-like crystals of complex **7** were obtained. The crystals were difficult to dissolve in water and common organic solvents except for DMSO and DMF. Yield: (based on Sm^{3+}): 50.3%. Analysis: (Anal. Calc. for $C_{48}H_{40}N_7O_7Sm$: C, 58.91; H, 4.05; N, 10.01%; Found: C, 58.94; H, 4.09; N, 10.03%). IR (KBr, ν, cm^{-1}):

3406(ν_{N-H}); 3057(δ_{Ar-H}); 2929, 2869($\nu_{-(CH2)-}$); 1586(ν_{asCOO-}); 1425(ν_{sCOO-}); 1518($\nu_{C=N}$); 1496 ($\nu_{C=C}$); 1385(ν_{NO3-}); 1190 (ν_{C-C}); 1102(ν_{C-N}); 1030(ν_{C-O}); 843, 746, 727(δ_{Ar-H}); 429(ν_{Sm-O}).

Complex Ln(IBA)$_3$(phen) (8-10) (Ln=Eu, Tb, Yb) A solution containing IBA (0.15 g, 0.75 mmol) and phen (0.05 g, 0.25 mmol) in ethanol (95%, 10 mL) was added drop-wise to a solution of $LnCl_3{\cdot}6H_2O$ (0.093 g, 0.25 mmol) in deionized water (10 mL). After the solution was left for 7 days at room temperature, light yellow needle-like crystals of complex 8-10 were obtained. The crystals were difficult to dissolve in water and common organic solvents except for DMSO and DMF.

$C_{48}H_{44}N_5O_6Eu$ (**8**): Yield: (based on Eu^{3+}): 56.9%. Analysis: (Anal. Calc. for $C_{48}H_{44}N_5O_6Eu$: C, 61.40; H, 4.61; N, 7.51%; Found: C, 61.35; H, 4.69; N, 7.46%). IR (KBr, ν, cm^{-1}): 3416(ν_{N-H}); 3048($_{Ar-H}$); 2947,2826($\nu_{-(CH2)-}$); 1579(ν_{asCOO-}); 1426(ν_{sCOO-}); 1516($\nu_{C=N}$); 1492($\nu_{C=C}$); 1195(ν_{C-C}); 1099(ν_{C-N}); 1031(ν_{C-O}); 864, 773, 746(δ_{Ar-H}); 421(ν_{Eu-O}).

$C_{48}H_{44}N_5O_6Tb$ (**9**): Yield: (based on Tb^{3+}): 53.1%. Analysis: (Anal. Calc. for $C_{48}H_{44}N_5O_6Tb$: C, 61.51; H, 4.58; N, 7.35%; Found: C, 60.90; H, 4.65; N, 7.40%). IR (KBr, ν, cm^{-1}): 3417(ν_{N-H}); 3045($_{Ar-H}$); 2947,2828($\nu_{-(CH2)-}$); 1580(ν_{asCOO-}); 1426(ν_{sCOO-}); 1517($\nu_{C=N}$); 1493($\nu_{C=C}$); 1193(ν_{C-C}); 1100(ν_{C-N}); 1034(ν_{C-O}); 870, 774 (δ_{Ar-H}); 424(ν_{Tb-O}).

$C_{48}H_{44}N_5O_6Yb$ (**10**): Yield: (based on Yb^{3+}): 49.6%. Analysis: (Anal. Calc. for $C_{48}H_{44}N_5O_6Yb$: C, 60.07; H, 4.62; N, 7.33%; Found: C, 60.00; H, 4.58; N, 7.29%). IR (KBr, ν, cm^{-1}): 3417(ν_{N-H}); 3050($_{Ar-H}$); 2945,2826($\nu_{-(CH2)-}$); 1579(ν_{asCOO-}); 1423(ν_{sCOO-}); 1515($\nu_{C=N}$); 1492($\nu_{C=C}$); 1199(ν_{C-C}); 1097(ν_{C-N}); 1033(ν_{C-O}); 862, 774, 746(δ_{Ar-H}); 419(ν_{Yb-O}).

X-ray crystallographic determination

Suitable single crystals of the ten complexes were mounted on glass fibers for X-ray measurement. Reflection data was collected at room temperature with a Bruker AXS SMART APEX II CCD diffractometer (Bruker AXS, Karlsruhe, Germany) with graphite-monochromated Mo-Ka radiation (λ = 0.71073 Å) and a ω scan mode. All measured independent reflections ($I > 2\sigma$ (I)) were used in the structural analysis and semi-empirical absorption corrections were applied using the SADABS program [12]. The structures were solved by the direct method using SHELXL-97 [13]. Crystal data and structure refinements are shown in Table 1-3. All non-hydrogen atoms were refined anisotropically and by temperature factor with the full-matrix least squares method. Hydrogen atoms of the organic frameworks were fixed at calculated positions with isotropic thermal parameters and refined using a riding model, whereas hydrogen atoms of the lattice water molecules were found in the Fourier different maps.

Result and discussion

Synthesis

By the solution preparation method, a series of Ln-IBA-phen complexes were successfully obtained for the first time. In the process, many factors may affect the crystallization and structure of the products, such as the starting reactants, pH value, solvent and temperature, etc. In our first attempt, we adopted the mixed solvent of methanol and H_2O with volume ratio 1: 1 in the system. Unfortunately, we only obtained some solid powder. Later, we replaced the solvent with the mixed ethanol and H_2O (1:1)/ (2:1) in the system, the products were all obtained. Moreover, the molar ratio of starting reactants was also play a key role in forming different structures of complexes. We attempted the molar ratio of $Ln(NO_3)_3{\cdot}6H_2O$, IBA and phen with 1: 3: 2 in the system, the complexes **1**-**6** were successfully obtained. After this, we replaced $Ln(NO_3)_3{\cdot}6H_2O$ with $LnCl_3{\cdot}6H_2O$ and adjusted the molar ratio ($m_{LnCl3\cdot6H2O}$:m_{IBA}: m_{phen}= 1: 3: 1) in the process of reaction, we gained the complex **8-10**, which was no free molecules in the structure (the binuclear building structure of complexes **6**, **7** and **10** shown in Fig.1). Following this, we wanted to know if it is possible to obtain some different structure from those complexes, so we adjusted various molar ratios and pH values. Fortunately, by using 1M NaOH to adjusting the pH value to 6 and with the molar ratio ($m_{Ln(NO3)3\cdot6H2O}$:m_{IBA}: m_{phen}= 1: 2: 2) in the reaction, complex **7** was successfully obtained. Additionally, the complexes were difficult to dissolve in water and common organic solvents except for DMSO and DMF.

Crystal structure

The structure of [Yb(IBA)$_3$(phen)]·(Hphen)·NO_3·2H_2O (6) Single-crystal X-ray structure analyses reveal that the frameworks of **1–6** are isomorphous, therefore, complex 6 is taken as an example to present and discuss the structure in detail. Structural analysis shows that the complex 6 was crystallized in the triclinic system with *P*-1 space group. The asymmetric unit of complex **6** consisted of one Yb atom, three IBA ligands, one coordinated phen ligand, one free phen molecule, one free NO_3 ion and two lattice H_2O molecules. The coordination environment of the central Yb(III) atom in complex **6** is shown in Fig. 2a with atom numbering. The Yb(III) atom is nine-coordinated by seven oxygen atoms (O1, O2, O3, O4, O5, $O4^{\#1}$ and $O6^{\#1}$, #1: 1-x, 1-y, 1-z) from five IBA ligands with Yb-O bond distances in the range of 2.253(2)-2.573(2) Å and two nitrogen atoms (N1 and N2) from one phen ligand with Yb-N distances in the range of 2.507(3)-2.562(3) Å to form a distorted tricapped trigonal prism geometry. In the structure of complex **6**, there are three types of coordination mode for the IBA ligands: a μ_2-η^1:η^1 double monodentate bridging mode (Scheme 1A), a μ_1-η^1:η^1 bidentate chelating mode (Scheme 1B) and a μ_2-η^1:η^2 bridging mode linking two lanthanide atoms (Scheme 1C).

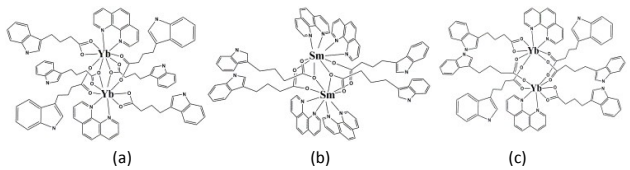

(a) (b) (c)

Fig 1. The molecular structure of complex **6** (a), **7** (b) and **10** (c).

Tab le 1 Summary of crystal data and refinement results for complexes 1-3*

Complexes	**1**	**2**	**3**
Formula	$C_{122}H_{116}N_{16}O_{21}La_2$	$C_{120}H_{114}N_{16}O_{22}Pr_2$	$C_{120}H_{114}N_{16}O_{22}Eu_2$
M ($g \cdot mol^{-1}$)	2420.13	2414.09	2436.19
Crystal system	Triclinic	Triclinic	Triclinic
Space group	*P*-1	*P*-1	*P*-1
a (Å)	13.729(3)	13.642(3)	13.549(4)
b (Å)	14.267(3)	14.294(3)	14.302(4)
c (Å)	16.791(3)	16.721(3)	16.740(5)
α (°)	79.44(3)	79.49(3)	79.802(4)
β (°)	71.27(3)	71.27(3)	71.163(4)
γ (°)	64.18(3)	64.01(3)	64.190(4)
V ($Å^3$)	2800.1(10)	2772.3(10)	2761.3(13)
Z	1	1	1
D_{calc} ($g \cdot cm^{-3}$)	1.435	1.446	1.465
Crystal size (mm)	0.42× 0.26 × 0.14	0.28× 0.20 × 0.16	0.32 × 0.18 × 0.15
F(000)	1242	1240	1248
μ(Mo-Kα)/ mm^{-1}	0.831	0.948	1.205
Reflections collected	22275	27020	15532
Independent reflections ($I > 2\sigma(I)$)	9856 (6605)	12540(10574)	11015(7949)
Parameters	737	721	731
Δ(ρ) (e $Å^{-3}$)	1.224 and -1.396	1.232 and -2.995	0.857 and -1.114
Goodness of fit	1.051	1.064	0.997
R_1[a]	0.0726 (0.1198)[b]	0.0534 (0.0653)[b]	0.0562 (0.0860)[b]
wR_2[a]	0.1265 (0.1525)[b]	0.1363 (0.1458)[b]	0.1080 (0.1232)[b]

[a] $R = \Sigma||Fo| - |Fc|| / \Sigma|Fo|$, $wR_2 = [\Sigma w(Fo^2 - Fc^2)^2 / [\Sigma w(Fo^2)^2]]^{1/2}$; [$Fo > 4\sigma(Fo)$].

[b] Based on all data.

Table 2 Summary of crystal data and refinement results for complexes 4-6*

Complex	**4**	**5**	**6**
Formula	$C_{120}H_{114}N_{16}O_{22}Gd_2$	$C_{120}H_{112}N_{16}O_{21}Tb_2$	$C_{120}H_{114}N_{16}O_{22}Yb_2$
M ($g \cdot mol^{-1}$)	2446.77	2432.12	2478.35
Crystal system	Triclinic	Triclinic	Triclinic
Space group	*P*-1	*P*-1	*P*-1
a (Å)	13.556(3)	13.519(5)	13.414(3)
b (Å)	14.326(3)	14.322(5)	14.310(3)
c (Å)	16.725(3)	16.732(6)	16.704(3)
α (°)	79.75(3)	79.854(6)	80.06(3)
β (°)	71.18(3)	71.098(6)	71.24(3)
γ (°)	64.16(3)	64.197(6)	64.17(3)
V ($Å^3$)	2764.3(10)	2757.0(17)	2730.7(10)
Z	1	1	1
D_{calc} ($g \cdot cm^{-3}$)	1.470	1.465	1.507
Crystal size (mm)	0.35× 0.20 × 0.17	0.35 × 0.18 × 0.12	0.32× 0.26 × 0.13
F(000)	1250	1242	1262
μ(Mo-Kα)/ mm^{-1}	1.269	1.351	1.783
Reflections collected	20994	8882	26539
Independent reflections ($I > 2\sigma(I)$)	10885(8051)	5336(3737)	12194(11252)
Parameters	721	721	721
Δ(ρ) (e $Å^{-3}$)	1.791 and -1.578	1.579 and -1.099	1.091and -0.690
Goodness of fit	1.030	1.000	1.070
R_1[a]	0.0760 (0.1055)[b]	0.0716 (0.1103)[b]	0.0264(0.0305)[b]
wR_2[a]	0.1748 (0.1965)[b]	0.1645 (0.1818)[b]	0.0808 (0.0893)[b]

[a] $R = \Sigma||Fo| - |Fc|| / \Sigma|Fo|$, $wR_2 = [\Sigma w(Fo^2 - Fc^2)^2 / [\Sigma w(Fo^2)^2]^{1/2}$; $[Fo > 4\sigma(Fo)]$.

[b] Based on all data.

Table 3 Summary of crystal data and refinement results for complexes 7-10*

Complex	**7**	**8**	**9**	**10**
Formula	$C_{96}H_{80}N_{14}O_{14}Sm_2$	$C_{96}H_{88}N_{10}O_{12}Eu_2$	$C_{96}H_{88}N_{10}O_{12}Tb_2$	$C_{96}H_{88}N_{10}O_{12}Yb_2$
M ($g \cdot mol^{-1}$)	1954.44	1877.68	1891.60	1919.84
Crystal system	Triclinic	Monoclinic	Monoclinic	Triclinic
Space group	*P*-1	*P*2(1)/*n*	*P*2(1)/*n*	*P*-1
a (Å)	11.7356(10)	13.811(3)	13.766(3)	10.887(2)
b (Å)	13.5161(11)	18.430(4)	18.430(4)	12.286(3)
c (Å)	13.8113(11)	17.214(3)	17.190(3)	16.566(3)
α (°)	101.229(2)	90	90	78.38(3)
β (°)	98.590(2)	106.47(3)	106.34(3)	86.60(3)
γ (°)	100.386(2)	90	90	71.74(3)
V ($Å^3$)	2074.6(3)	4201.7(15)	4185.2(15)	2061.1(7)
Z	1	2	2	1
D_{calc} ($g \cdot cm^{-3}$)	1.564	1.484	1.501	1.547
Crystal size (mm)	0.18 × 0.11 × 0.06	0.43 × 0.32 × 0.30	0.24× 0.16 × 0.09	0.20× 0.14 × 0.06
F(000)	990	1912	1920	970
μ(Mo-Kα)/ mm^{-1}	1.479	1.549	1.746	2.326
Reflections collected	11109	39507	37765	16326
Independent reflections ($I > 2\sigma(I)$)	7226(6059)	9560(6495)	9467(6445)	7236(5152)
Parameters	587	541	541	541
Δ(ρ) (e $Å^{-3}$)	1.197 and -0.694	0.664 and -1.157	0.978 and -1.479	3.325 and -2.615
Goodness of fit	1.035	1.013	1.038	1.051
R_1[a]	0.0498 (0.0625)[b]	0.0485 (0.0890)[b]	0.0613 (0.1035)[b]	0.0951 (0.1328)[b]
wR_2[a]	0.1060 (0.1247)[b]	0.0745 (0.0833)[b]	0.0912 (0.1056)[b]	0.19.58 (0.2213)[b]

[a] $R = \Sigma||Fo| - |Fc|| / \Sigma|Fo|$, $wR_2 = [\Sigma w(Fo^2 - Fc^2)^2 / [\Sigma w(Fo^2)^2]]^{1/2}$; [$Fo > 4\sigma(Fo)$].

[b] Based on all data.

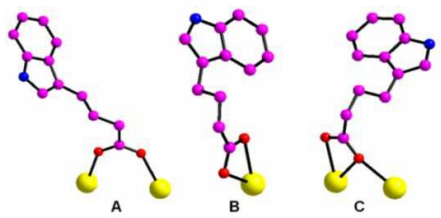

Scheme 1 Coordination modes of IBA ligand

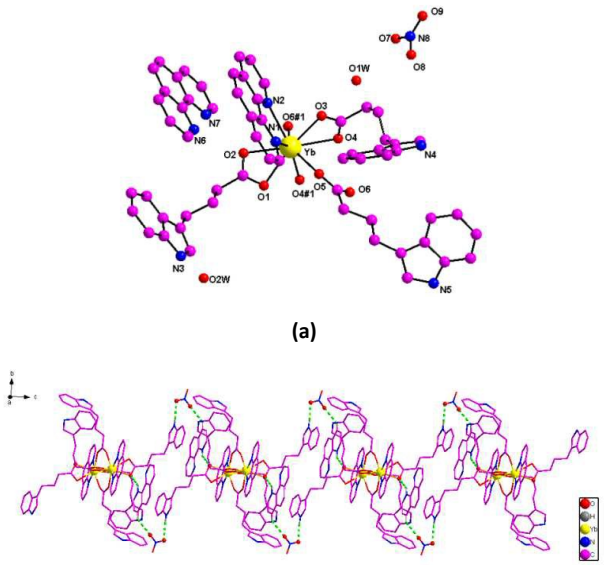

Fig. 2. (a) The unit structure of complex **6** (symmetric code: #1: 1-x, 1-y, 1-z); (b) A view of 1D chain structure via hydrogen bonds along the *c*-axis (#2: -1+x, 1+y, 1+z; #3: x, 1+y, z; #4: 1-x, -y, 1-z).

Adjacent Yb atoms are linked via the μ_2-bridging carboxylate groups of the IBA ligands to generate a binuclear building unit. There are two types of hydrogen bonds in complex 6: (i) N-H···O (N7-H7···O2, N3-H3A···O9$^{\#2}$, N5-H5A···O1W$^{\#3}$, #2: -1+x, 1+y, 1+z; #3: x, 1+y, z); (ii) C-H···O (C56-H56A···O7$^{\#4}$, #4: 1-x, -y, 1-z). The binuclear building unit were connected by the hydrogen of N3-H3A···O9$^{\#2}$ between the nitrogen atom from IBA ligand and the oxygen atom from free NO_3^- ion, C56-H56A ···O7$^{\#3}$ between the carbon atom from free Hphen and the oxygen atom from free NO_3^- ion and N7-H7···O2 between nitrogen atom from free Hphen and the oxygen atom from IBA ligand to form a 1D chain structure along the *c*-axis (Fig. 2b)Additionally, the molecules were furthermore stabilized by the hydrogen bonding interactions of N5-H5A···O1W$^{\#3}$.

The structure of $[Sm(IBA)_2(phen)_2]\cdot NO_3$ (7) X-ray diffraction analysis revealed that the asymmetric unit of complex 7 consisted of one Sm atom, two IBA ligands, two phen ligands and one free NO^{3-} ion. The coordination environment of the central Sm(III) atom is shown in Fig. 3a with atom numbering. The Sm(III) atom is nine-coordinated by five oxygen atoms (O1, O3, O4, O2$^{\#1}$ and O4$^{\#1}$, #1: -x, -y, 1-z.) from four IBA ligands with Sm-O bond distances in the range of 2.350(4)-2.588(4) Å and four nitrogen atoms (N1, N2, N3 and N4) from two phen ligands with Sm-N distances in the range of 2.621(4)-2.666(5) Å to form a distorted tricapped trigonal prism geometry. In the structure of complex 7, there are two types of coordination mode for the IBA ligand: a μ_2-η^1:η^2 bridging mode linking two lanthanide atoms (Scheme 1C) and a μ_2-η^1:η^1 double monodentate bridging mode (Scheme 1A). Adjacent Sm atoms are linked via the μ_2-bridging carboxylate groups of the IBA ligands to generate a binuclear building unit. The binuclear units are further connected through hydrogen bonds of C17$^{\#4}$-H17A···O3 (#4: 1-x, 1-y, 1-z) between the carbon atom from the phen ligand and oxygen atom from the IBA ligand to form a 1D hydrogen-bonding chain along the b-axis (Fig. 3b). Furthermore, by the hydrogen bonds of N5$^{\#2}$-H5A···O6 (#2: x+1, y, z+1) and N6$^{\#3}$-H6A···O6 (#3: x, y, z+1) between the nitrogen atom from IBA ligand and oxygen atom from free NO_3^- ion to form a 2D supramolecular network structure (Fig. 3c).

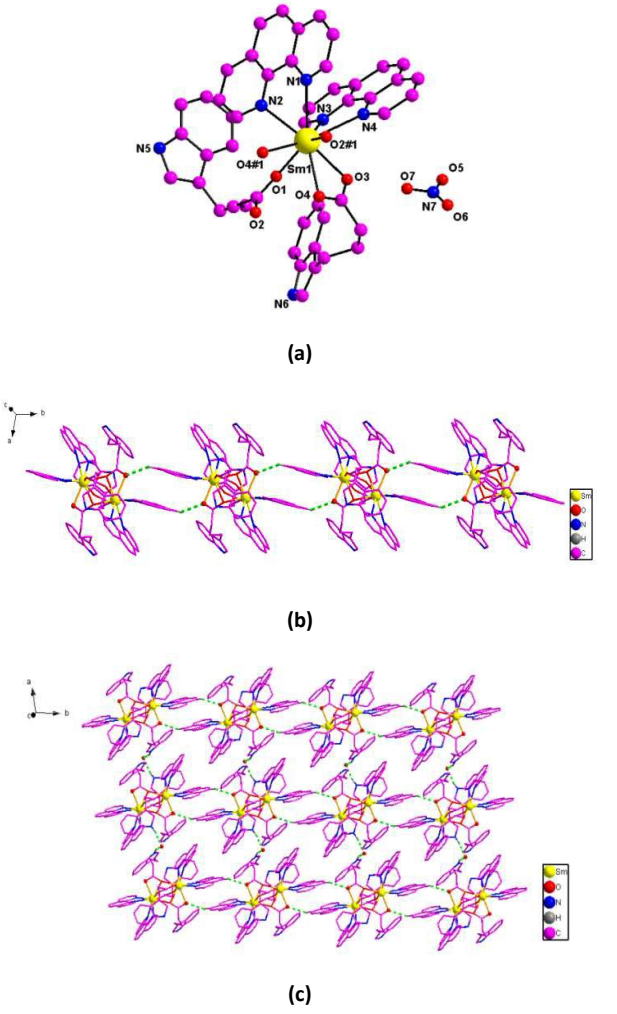

Fig 3. (a) The unit structure of complex **7** (symmetric code: #1: -x, -y, 1-z); (b) A view of 1D chain via hydrogen bonds along the *b*-axis (symmetry code:#4: 1-x, 1-y, 1-z); (c) A view of 2D network structure via hydrogen bonds along the *ab* plane(symmetry code: #2: x+1, y, z+1; #3: x, y, z+1).

The structure of Eu(IBA)$_3$(phen) (8) Single-crystal X-ray structure analyses reveal that the frameworks of **8–10** are isomorphous, therefore, complex **8** is taken as an example to present and discuss the structure in detail. X-ray diffraction analysis revealed that the asymmetric unit of complex **8** consisted of one Eu atom, three IBA ligands and one phen ligand. The coordination environment of the central Eu(III) atom in complex **8** is shown in Fig. 4a with atom numbering. The Eu(III) atom is nine-coordinated by seven oxygen atoms (O1, O2, O3, O4, O5, O4$^{\#1}$ and O6$^{\#1}$, #1: -x, -y, 1-z) from five IBA ligands with Eu-O bond distances in the range of 2.355 (3)-2.618 (3) Å and two nitrogen atoms (N1 and N2) from one phen ligand with Eu-N distances in the range of 2.618 (4)-2.621 (3) Å, to form a distorted tricapped trigonal prism geometry. In the structure of complex **8**, there are three types of coordination mode for the IBA ligand: a μ_2-η^1:η^1 double monodentate bridging mode (Scheme 1A), a μ_1-η^1:η^1 bidentate chelating mode (Scheme 1B) and a μ_2-η^1:η^2 bridging mode linking two lanthanide atoms (Scheme 1C). Adjacent Eu atoms are linked via the μ_2-bridging carboxylate groups of the IBA ligands to generate a binuclear building unit. The binuclear units are further connected through hydrogen bonds of N3$^{\#2}$-H3A$\cdots$O3 (#2: 1/2-x, y-1/2, 1/2-z) between the nitrogen atom and coordinated oxygen atom from IBA ligand to form a 2D network structure along *ab* plane (Fig. 4b). Furthermore, by the hydrogen bonds of N4$^{\#3}$-H4A$\cdots$O2 (#3: 1/2-x, y+1/2, 3/2-z) between the nitrogen atom and coordinated oxygen atom from the IBA ligand to form a 3D supramolecular structure (Fig. 4c).

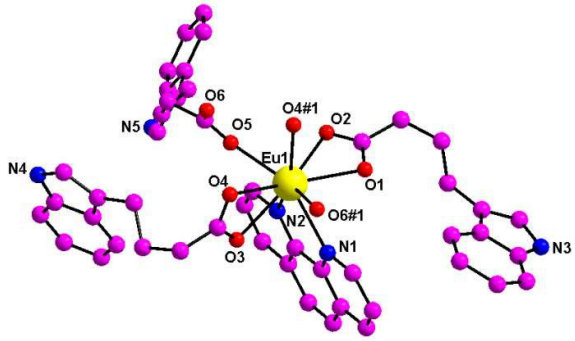

(a)

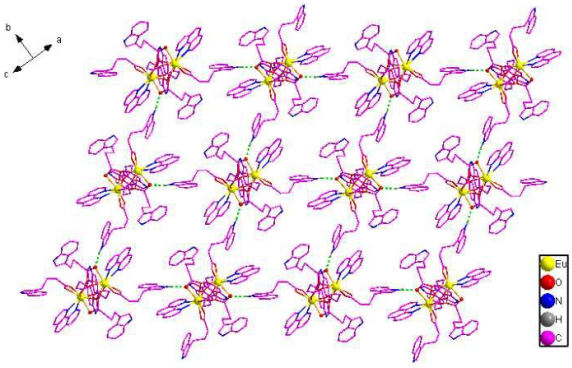

(b)

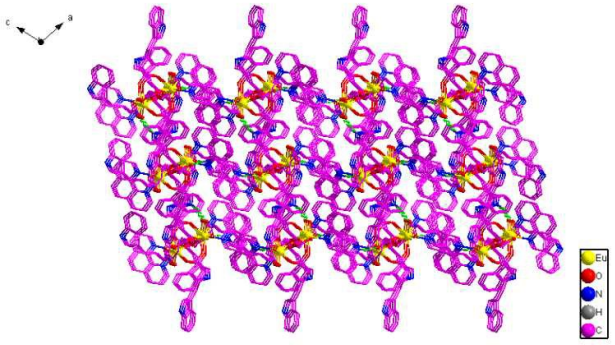

(c)

Fig. 4. (a) The unit structure of complex **8** (symmetric code: #1: -x, -y, 1-z); (b) A view of 2D network structure via hydrogen bonds along the *ab* plane (symmetry code: #2: 1/2-x, y-1/2, 1/2-z); (c) A view of 3D supramolecular structure via hydrogen bonds (symmetry code: #3: 1/2-x, y+1/2, 3/2-z).

By comparison, the lanthanide atom in complex **6**, **7** and **8** were all nine-coordinated to form distorted tricapped trigonal prism geometry. As for those complexes, they contain the same IBA ligand, but the coordination mode of IBA ligand is different. In complexes **6** and **8**, there are three kinds of coordination mode of IBA ligand: a μ_2-η^1:η^1 double monodentate bridging mode (Scheme 1A), a μ_1-η^1:η^1 bidentate chelating mode (Scheme 1B) and a μ_2-η^1:η^2 bridging mode linking two lanthanide atoms (Scheme 1C). However in complex **7**, two kinds of coordination mode of IBA ligand: a μ_2-η^1:η^2 bridging mode linking two lanthanide atoms (Scheme 1C) and a μ_2-η^1:η^1 double monodentate bridging mode (Scheme 1A) was observed. Additionally, by the hydrogen bonding interactions, complexes **6, 7** and **8** were connected by the hydrogen bond to form 1D, 2D and 3D supramolecular network structures, respectively.

IR spectra

For complex **6**, the absorption bands appearing at 1586 cm^{-1} and 1429 cm^{-1} are assigned to the asymmetric stretching vibrations and symmetric stretching vibrations of the carboxylate groups, while the characteristic bands of asymmetric and symmetric stretching vibrations of the carboxylate groups in free IBA are 1696 cm^{-1} and 1456 cm^{-1}, respectively. The analysis shows that oxygen atoms on the carboxylate groups of the ligand are involved in coordination with the metal atom. The absorption band appearing at 1516 cm^{-1} is assigned to the stretching vibrations of $\nu_{C=N}$ in the complex, in contrast to the characteristic band of free phen (1586 cm^{-1}), showing that phen participates to the coordination with the metal atom. The absorption band at 3407 cm^{-1} may be assigned to the stretching vibrations of N-H in the IBA ligand. The absorption band at 1385 cm^{-1} represents the stretching vibration of N-O from the NO_3^- ion lattice. The detailed IR spectra data for complexes **6**, **7** and **8** are shown in Table S5. The IR spectra of all complexes are listed in Fig. S1-S10.

UV-vis spectra

The UV-visible absorption spectra of complexes **1**-**10** are shown in Fig. S11-S20. The detailed assignments of these

complexes were listed in Table S6. The peaks appearing at about 214 and 260 nm are attributed to π→π* transition of the ligand. For the lanthanide atoms of complexes **2**, **6**, **7** and **10**, f→f* transitions peaks are present in the visible light, infrared and far-infrared region. But for other complexes, the f→f* transitions peaks were not observed in the spectra.

Photoluminescence spectra

Lanthanide complexes have attracted considerable attention as promising sensory materials due to their intense luminescence [14]. The luminescent behaviours of complexes **3**, **5** and **8** were investigated in the solid state at room temperature (Fig. S21-S23). When excited at 397 nm for **3** and 365 nm for **8**, they emitted red light at room temperature. The emission peaks of complexes correspond to the transitions from $^5D_0 \rightarrow {}^7F_n$ (n = 1, 2, 3 and 4) transitions at 592, 596, 615, 650 and 685 nm for Eu (III) ion in complex **3** and at 593, 617, 654, 689 and 699 nm for Eu (III) in complex **8**, respectively. Among these transitions, $^5D_0 \rightarrow {}^7F_2$ is the strongest [15]. For complex **5**, upon excitation at 349 nm, the relatively emissions were observed, which corresponds to the $^5D_4 \rightarrow {}^7F_n$ transitions at 489, 546, 585 and 621 nm for n=6, 5, 4 and 3, respectively. The most prominent line was observed at 546 nm.

Thermal Properties

To examine the thermal stability of the complexes, thermal gravimetric analysis (TG) were carried out at a heating rate of 10 ^oC/min under the condition of N_2 atmosphere with the temperature ranging from 20 to 1000 ^oC (Fig. S24-S33). TG curve of complex **6** showed the thermal decomposition process can be divided into two stages. The first weight loss of 2.70% between 20 and 120 ^oC corresponds to the loss of two lattice H_2O molecules (calc. 2.99%). The second weight loss occurring in the temperature range of 120-1000 °C should be ascribed to the release of one free NO_3^- molecule, one free Hphen group, one coordinated phen molecule and three coordinated IBA ligands (obsd. 81.18%, calc. 81.11%). Finally the remaining weight corresponds to the formation of Yb_2O_3 (obsd. 16.12%, calc. 15.90%). For complex **7**, the TG curve is divided into three steps. The first weight loss of 6.40% in the range of 88 to 233°C should be attributed to one free NO_3^- (calc. 6.34%). The second weight loss occurs in the range of 234-315°C, with a percentage weight loss of 41.15% (calc. 40.50%), which is ascribed to the release of two phen ligands. The last step of decomposition occurred within the range of 320 to 1000°C, which is considered the loss of one and a half IBA ligand, and the final residue is corresponding to Sm_2O_3 (obsd. 18.00%, calc. 17.84%). The TG curve of complex **8** shows only one stage. the weight loss of 81.44% (calc. 81.26%) in the range of 243-1000°C should be attributed to the release of one phen ligand and three IBA ligands, the final residue is corresponding to Eu_2O_3 (obsd. 18.56%, calc. 18.74%).

PXRD analysis

The powder X-ray diffraction data of the complexes **1**-**10** were obtained and compared with the corresponding simulated single-crystal diffraction data (Fig.S34-S43). The phase of the corresponding complex is considered as purities owning to the agreement of the peak positions. The different intensity may be due to the preferred orientation of the powder samples.

Antimicrobial activity

The antimicrobial activities of all the tested complexes are presented in Table 4. To investigate the antimicrobial activated component of the complexes, we have used the $Ln(NO_3)_3{\cdot}6H_2O$, IBA and phen as antibacterial agent, respectively, and the results shown that neither the $Ln(NO_3)_3{\cdot}6H_2O$ nor the IBA exhibited the antibacterial activity (the antibacterial effects of $La(NO_3)_3$ and IBA against the C.A were shown in Fig.5, and those of $Pr(NO_3)_3$ and IBA against the B.S were shown in Fig.6). However, the 1,10-phen ligand and the complexes exhibit broad spectrum antimicrobial activity against all the five chosen reference bacteria [16]. And the antimicrobial activities of 1,10-phen ligand was much better than the metal complexes under the same concentration (Fig.7). It is known that the amount of the 1, 10-phen ligand is much higher than those in complexes. For complexes **1**-**6**, the amount of the 1, 10-phen is 6.15-0.75 mg/ml, so we selected four different concentrations (6.15, 3.1, 1.6 and 0.8 mg/ml) of 1,10-phen to test the antimicrobial activities of the five bacteria(Table 4 for phen 1). Similarly, for complex **7** and complexes **8**-**10**, we also selected the four different concentrations 7.34, 3.67, 1.8, 0.92 mg/ml and 3.83, 1.92, 0.96, 0.48 mg/ml of 1,10-phen to test the antimicrobial activities of the five bacteria, respectively (Table 4 for phen 2 and phen 3).

Table 4 Antimicrobial activity of complexes 1-10 and ligand

No.	Dose (µg/ml)	n_{phen} (mol)	Diameter of zone (mm)				
			G.S	E.C	P.A	C.A	B.S
	200	1.11E-06	22.2	25.7	27.4	27	29.5
	100	5.55E-07	18.7	22.5	23.2	23.5	27.0
phen	50	2.77E-07	16.3	19.4	20.5	19.8	22.2
	25	1.39E-07	13.0	15.0	16.2	15.0	16.8
	12.5	6.95E-08	8	8.8	11.1	10.2	11.3
	6.25	3.48E-08	0	0	0	0	0
		R^2	0.9513	0.9546	0.9371	0.9503	0.9511
	200	3.42E-07	18.6	21.5	21.3	20.8	22.6
	100	1.71E-07	14.2	18.6	18.1	18.0	18.3
1	50	8.6 E-08	8.8	14.3	13.8	14.9	13.8
	25	4.3 E-08	6.0	10.3	9.6	8.8	8.8
		R^2	0.9720	0.9980	0.9990	0.9612	0.9991
	200	3.42E-07	16.8	21.5	20.8	22.0	23.7
	100	1.71E-07	14.8	18.6	17.8	18.9	19.3
2	50	8.6 E-08	8.8	15.7	15.3	16	15.8
	25	4.3 E-08	6.7	12.3	10.4	11.3	11.7
		R^2	0.9516	0.9990	0.9890	0.9865	0.9921
	200	3.38E-07	16.7	22.5	22.0	22.4	21.3
	100	1.69E-07	12.5	19.0	16.7	21.0	16.5
3	50	8.45E-08	7.4	15.0	11.5	16.8	10.4
	25	4.22E-08	6.5	8.0	7.7	10.9	6.0
		R^2	0.9122	0.9875	0.9816	0.936	0.9902
	200	3.37E-07	16.7	21.0	20.5	20.7	19.8
	100	1.69E-07	14.1	17.9	17.1	16.5	14.2
4	50	8.45E-08	6.8	13.9	12.7	12.8	10.6
	25	4.22E-08	6.3	9.4	8.7	9.0	6.9
		R^2	0.9355	0.9996	0.9979	0.9999	0.9710
	200	3.36E-07	16.8	21.0	22.3	21.4	23.6
	100	1.68E-07	12.1	18.6	18.4	17.3	17.3
5	50	8.40E-08	7.2	14.2	14.5	13.3	14.2
	25	4.20E-08	6.0	8.5	10.0	9.1	8.9
		R^2	0.9189	0.9876	0.9988	0.9930	0.9750
	200	3.32E-07	15.2	17.4	18.0	15.3	18.3
	100	1.66E-07	11.5	12.7	13.9	12.8	12.3
6	50	8.30E-08	6.8	9.2	9.7	8.9	7.7
	25	4.15E-08	6.0	6.9	6.8	6.0	6.6
		R^2	0.9128	0.9541	0.9806	0.9936	0.8908
	200	4.05E-07	23.3	24.0	24.0	25.3	29.3
	100	2.03E-07	17.0	20.0	21.3	21.0	21.7
7	50	1.01E-07	12.8	15.0	17.8	17.3	15.7
	25	5.06E-08	6.0	11.0	11.8	13.0	13.8
		R^2	0.9930	0.9978	0.9811	0.9992	0.9407
	200	2.13E-07	16.1	20.0	19.0	20.0	20.0
	100	1.07E-07	13.0	15.3	15.0	14.3	14.0
8	50	5.33E-08	6.7	8.8	7.0	7.9	9.0
	25	2.66E-08	6.0	7.0	6.0	6.0	6.0
		R^2	0.9135	0.9617	0.9314	0.9599	0.9797
	200	2.11E-07	16.0	19.0	20.0	18.0	21.0
	100	1.06E-07	14.0	15.3	14.7	14.7	13.7
9	50	5.28E-08	6.7	10.7	10.3	7.9	9.7
	25	2.64E-08	6.0	6.0	6.0	6.0	6.3
		R^2	0.9269	0.9971	0.9973	0.9591	0.9647
	200	2.08E-07	15.3	17.7	19.0	18.3	18.3
	100	1.04E-07	12	13.7	14.7	13.7	12.7
10	50	5.20E-08	6.7	7.7	8.0	10.0	8.0
	25	2.60E-08	6	6.0	6.0	6.0	6.0
		R^2	0.9355	0.9632	0.9654	0.9979	0.9624

	61.5	3.41E-07	16.8	19.9	21.5	20.4	22.5
phen 1	30.8	1.71E-07	13.2	15.2	16.4	15.8	17.9
	15.4	8.53E-08	8.8	10	11.6	10.5	11.2
	7.70	4.27E-08	6.0	6	6.1	6	6
	73.4	4.07E-07	18.2	21.1	22.9	21.7	23.9
phen 2	36.7	2.04E-07	13.8	16.2	17.7	16.7	18.2
	18.4	1.02E-07	9.2	11.3	12.6	11.8	12.6
	9.18	5.09E-08	6.7	6.0	7.4	6.9	7.0
	38.3	2.13E-07	14.3	16.6	18.1	17.0	18.7
phen 3	19.2	1.06E-07	10.2	11.6	12.9	12.1	13.0
	9.58	5.31E-08	6	6.7	7.7	7.2	7.5
	4.79	2.66E-08	0	0	0	0	0
	200		0	0	0	0	5.2
IBA	100		0	0	0	0	5.2
	50		0	0	0	0	5.2
	25		0	0	0	0	0

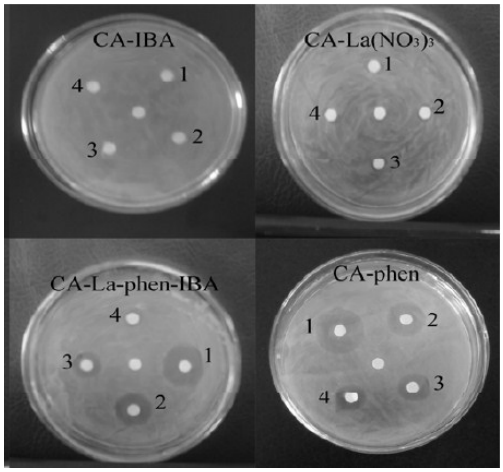

Fig. 5 Antibacterial effects of complexes 1, $La(NO_3)_3$ and ligand on C.A (1) 20 mg/ml (2) 10 mg/ml (3) 5 mg/ml (4) 2.5 mg/ml

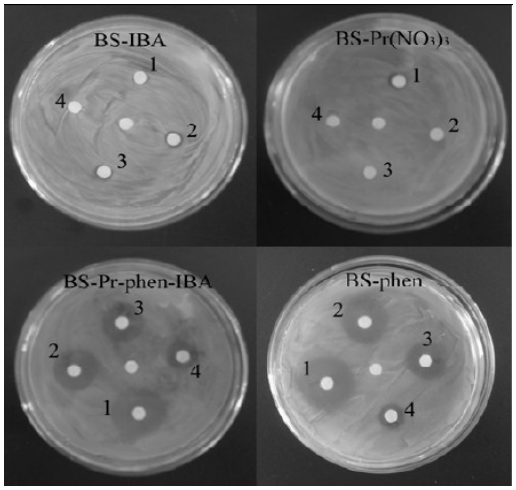

Fig. 6 Antibacterial effects of complexes **2**, $Pr(NO_3)_3$ and ligand on B.S (1) 20 mg/ml (2) 10 mg/ml (3) 5 mg/ml (4) 2.5 mg/ml

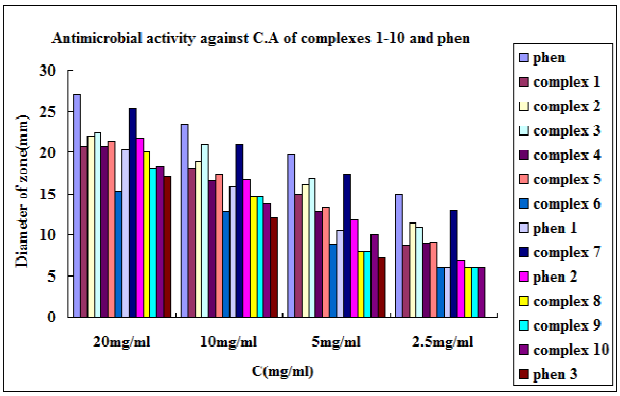

Fig. 7 Antimicrobial activity against C.A of complexes 1-10 and phen (**phen 1**: 6.15 mg/ml, 3.08 mg/ml, 1.54 mg/ml, 0.77 mg/ml; **phen 2**: 7.34 mg/ml, 3.67 mg/ml, 1.84 mg/ml, 0.92 mg/ml; **phen 3**: 3.83 mg/ml, 1.92 mg/ml, 0.96 mg/ml, 0.48 mg/ml)

From the results given in Table 4, it has been observed that all selected complexes show antimicrobial activities against the five bacteria, and their antimicrobial activities was ordered as: complex **7** > complexes **1**-**5** > complex **6** > complexes **8**-**10**. This would imply that the higher amount of 1, 10-phen in complex could enhance the antimicrobial activities. Moreover, against the bacteria B. S, the complexes **1**, **2**, **5**, **6** and **9** are more active than other complexes. Complexes **4** and **5** exhibit antimicrobial activity against the bacteria E.C. In addition, against the bacteria P.A, complex **10** are more active than other complexes (Table 5). From the results given in Table 4, it has been observed that the diameters of the inhibition zones with the relative amounts of phen existing linear relationship (Fig8-10), and the R^2 are all above 0.9. Additionally, the straight lines which are above the dotted lines indicating that those complexes exhibit more active antimicrobial activities than 1,10-phen under the same amount of 1,10-phen. While the antimicrobial activity of these light lanthanide complexes (La, Pr, Sm, Eu) are more effective than that of heavy lanthanide complexes (Gd, Tb, Yb) [17].

In order to explore the antimicrobial mechanism of such complexes, we chose the complex 2 as the research object

with the Agarose gel electrophoresis method to determine and quantify the products cleavaged from *E. Coli* DNA. Gel electrophoresis pictures (Fig 11) are shown in control experiments clearly revealed that complex **2** cleaves *E. Coli* DNA with dose-response relationship. When the sample is 6 mg/ml, the DNA show slightly cleavage (Fig 11, Lane 3), however, the DNA was complete cleavage when the sample is 10 mg/ml (Fig 11, Lane 5). So further experiment results indicated that complexes might potentially inhibit the growth of bacteria by braking the DNA of bacteria [18].

Table 5 The comparisons of antimicrobial activities of complexes 1-10 against different bacterium

Complexes	The order of the antimicrobial activities
1	B.S > C.A > E.C > P.A > G.S
2	B.S > E.C > P.A > C.A > G.S
3	E.C > C.A > P.A > B.S > G.S
4	E.C > P.A > C.A > B.S > G.S
5	B.S > P.A > C.A > E.C > G.S
6	B.S > P.A > E.C > C.A > G.S
7	B.S > C.A > P.A > E.C > G.S
8	E.C > C.A > B.S > P.A > G.S
9	B.S > P.A > E.C > G.S > C.A
10	P.A > C.A > B.S > E.C > G.S

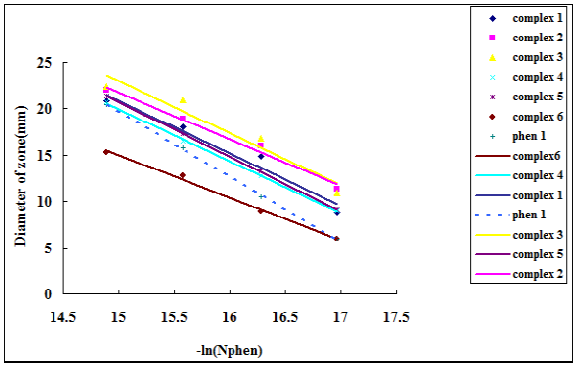

Fig. 8 The associations of the diameters of the inhibition zones with relative amounts of phen in complexes **1**-**6** against C.A

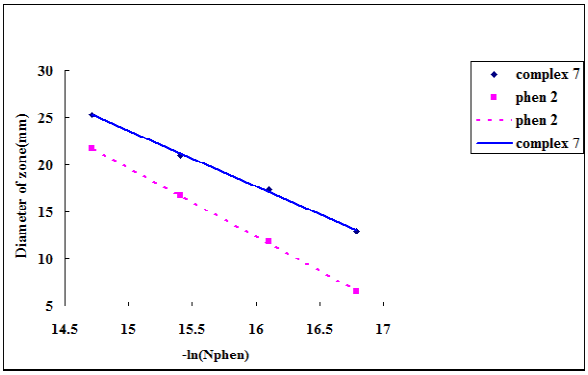

Fig. 9 The associations of the diameters of the inhibition zones with relative amounts of phen in complex **7** against C.A

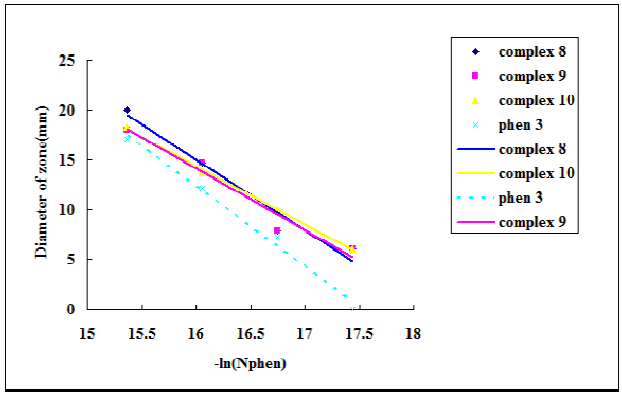

Fig. 10 The associations of the diameters of the inhibition zones with relative amounts of phen in complex **8-10** against C.A

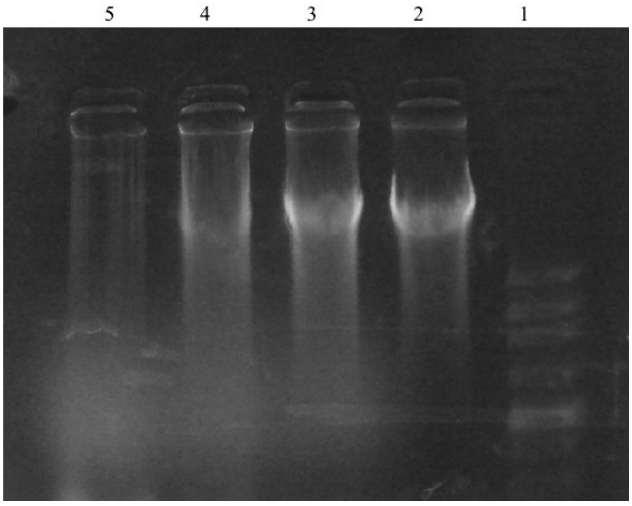

Fig. 11 Agarosegel eletrophoresis of Escherichia coli DNA cleaved by complex **2** Lane 1: Marker; Lane 2: Normal DNA; Lane 3: Incutated with complex **2** (6mg/ml); Lane 4: Incubated with complex **2** (8mg/ml); Lane 5: Incubated with complex **2** (10mg/ml)

Conclusions

In summary, by using IBA and 1,10-phen mixed organic ligands, a series of novel lanthanide complexes have been synthesized and characterized. All complexes were characterized by elemental analysis, IR spectroscopy, and single-crystal X-ray diffraction. The complexes exhibit broad spectrum antimicrobial activity against all the five chosen reference bacteria, and the antimicrobial activity of light lanthanide complexes (La, Pr, Sm, Eu) are more effective than that of heavy lanthanide complexes (Gd, Tb, Yb). Agarose gel electrophoresis was performed to determine that complexes might potentially inhibit the growth of bacteria by braking the DNA of bacteria. So those complexes exhibiting antimicrobial activity, may be developed as new antimicrobial agents.

Acknowledgements

This work was supported by the grants of the National Natural Science Foundation of China (Grant No. 21371086, 21571091).

References

1. H. V. Goulding, S. E. Hulse, W. Clegg, R. W. Harrington, H. Y. Playford, R. I. Walton and A. M. Fogg, *J. Am. Chem. Soc.*, 2010, **132**, 13618; G. J. Halder, C. J. Kepert, M. Boujemaa, K. S. Murray and J. D. Cashion, *Science*, 2002, **298**, 1762; T. K. Maji, P. S. Mukherjee, N. R. Chaudhuri, G. Mostafa and E. Zangrando, *Chem. Commun.*, 2001, **15**, 1368; K. O, *Acc.chem.res*, 2000, **33**, 647; J. Yu and R. Xu, *Chem. Soc. Rev.*, 2006, **35**, 593.
2. T. Devic, Christian Serre, N. Audebrand, J. Marrot and G. Férey, *J. Am. Chem. Soc.*, 2005, **127**, 12788.
3. R. S. Zhou, L. Ye, H. Ding, J. F. Song, X. Y. Xu and J. Q. Xu, *J. Solid State Chem.*, 2008, **181**, 567.
4. R. Nathaniel L, K. Jaheon, E. Mohamed, C. Banglin, O. K. Michael and Y. Omar M, *J. Am. Chem. Soc.*, 2005, **127**, 1504.
5. G. X, Z. G, L. Z, S. F, Y. Z and Q. S, *Chem. Commun.*, 2006, **30**, 3172.
6. B. Chen, Y. Yang, F. Zapata, G. Lin, G. Qian and E. B. Lobkovsky, *Adv. Mater.*, 2007, **19**, 1693.
7. L. A. Borkowski and C. L. Cahill, *Acta Crystallogr.*, 2004, **60**, 159.
8. F. N. Shi, L. Cunha-Silva, R. A. S. Ferreira, L. Mafra, T. Trindade, L. D. Carlos, F. A. A. Paz and J. Rocha, *J.am.chem.soc*, 2007, **130**, 150.
9. J. Ludwig-Muller, *Plant Growth Regulation*, 2000, **32**, 219.
10. C. T. Dillon, H. T. BJ, P. A. Lay, Q. Zhou, N. M. Davies, J. R. Biffin and H. L. Regtop, *Chem.res.toxicol*, 2003, **16**, 28; Q. L. Guan, Y. H. Xing, L. Jing, W. J. Wei, Z. Rui, W. Xuan and F. Y. Bai, *J. Inorg. Biochem.*, 2013, **128**, 57; W. Je., K. Bj., L. Pa., D. Maclachlan, B. R. D. Cd., M. Ks., B. Moubaraki, B. Warwick, B. Jr. and R. Hl., *Inorg. Chem.*, 1999, **38**, 1736; Z. Qingdi, T. W. Hambley, B. J. Kennedy and P. A. Lay, *Inorg. Chem.*, 2003, **42**, 8557; J. E. Weder, T. W. Hambley, B. J. Kennedy, P. A. Lay, G. J. Foran and A. M. Rich, *Inorg. Chem.*, 2001, **40**, 1295; R. M. Ying, P. Turner, B. J. Kennedy, T. W. Hambley, P. A. Lay, J. R. Biffin, H. L. Regtop and B. Warwick, *Inorg. Chim. Acta*, 2001, **324**, 150; Q. Zhou, T. W. Hambley, B. J. Kennedy, P. A. Lay, P. Turner, B. Warwick, J. R. Biffin and R. HL, *Inorg. Chem.*, 2000, **39**, 3742.
11. R. Feng, C. Wei and S. Tu, *Environ. Exp. Bot.*, 2013, **87**, 58; Z. Hu, H. Richter, G. Sparovek and E. Schnug, *J. Plant Nutr.*, 2004, **27**, 183; L. Wang, J. Li, Q. Zhou, G. Yang, X. L. Ding, X. Li, C. X. Cai, Z. Zhang, H. Y. Wei and T. H. Lu, *Proc. Natl. Acad. Sci. U. S. A.*, 2014, **111**, 12936.
12. G. i. Sheldrick, *University of Göttingen, Germany*, 1996.
13. G. M. Sheldrick, *University of Göttingen, Germany*, 1997, 1456.
14. W. Nicolas, L. C. J. Charbonnière, G. Massimo, R. Aldo and Z. Raymond, *J.am.chem.soc*, 2004, **126**, 4888; P. Stéphane, S. M. Cohen, J. C. G. Bünzli and K. N. Raymond, *J. Am. Chem. Soc.*, 2003, **125**, 13324.
15. K. L. Hou, F. Y. Bai, Y. H. Xing, J. L. Wang, Z. Shi, K. L. Hou, F. Y. Bai, Y. H. Xing, J. L. Wang and Z. Shi, *Inorg. Chim. Acta*, 2011, **365**, 269; X. J. Zhang, Y. H. Xing, Z. Sun, J. Han, Y. H. Zhang, M. F. Ge and S. Y. Niu, *Cryst. Growth Des.*, 2007, **7**, 2041.
16. Y. Lin, T. Dongliang, Y. Xiaoli, L. Yongfang and G. Yuming, *Chem. Pharm. Bull. (Tokyo)*, 2003, **51**, 494; N. C. Saha, S. Mandal, M. Das, N. Khatun, D. Mitra, A. Samanta, A. M. Z. Slawin, R. J. Butcher and R. Saha, *Polyhedron*, 2014, **68**, 122.
17. Marina Juribašića, Krešimir Molčanova, Biserka Kojić-Prodića, Lisa Bellottob, Marijeta Kraljc, Franca Zanid and L. Tušek-Božića, *J. Inorg. Biochem.*, 2011, **105**, 867; G. Nirmala, A. K. Rahiman, S. Sreedaran, R. Jegadeesh, N. Raaman and V. Narayanan, *Polyhedron*, 2011, **30**, 106.
18. A. Kulkarni, S. A. Patil and P. S. Badami, *Eur. J. Med. Chem.*, 2009, **44**, 2904; Tajmir-Riahi HA, Ahmad R and N. M., *J. Biomol. Struct. Dyn.*, 1993, **10**, 865; L. Tušek-Božić, M. Komac, Manda Ćurića, Antonin Lyčkab, Martina D'Alpaosc, Vito Scarciad and A. Furlanid, *Polyhedron*, 2000, **19**, 937.

Synthesis, crystal structure, fluorescence and antimicrobial activity of a series of rare-earth complexes based on indolebutyric acid

Zhi-Nan Wang,[a] Xue-Ting Xu,[a] Xiao Lv,[b] Feng-Ying Bai,[a*] Shu-Qing Liu[b*] and Yong-Heng Xing[a]

[a] College of Chemistry and Chemical Engineering Liaoning Normal University, Dalian, 116029, P. R. China. E-mail: baifengying2003@163.com

[b] Department of Biochemistry and Molecular Biology, Dalian Medical University, Dalian, 116044, P. R. China. E-mail: Lsqsmz@163.com

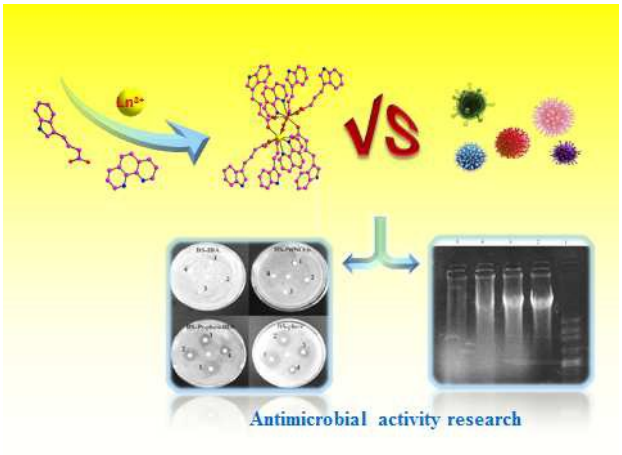

Antimicrobial activity of a series of rare earth complexes were investigated in detail.